21th International Conference on Renewable Energies and Power Quality (ICREPQ'23)
Madrid (Spain), 24th to 26th May 2023
Renewable Energy and Power Quality Journal (RE&PQJ)
ISSN 2172-038 X, Volume No.21, July 2023

# Optimal active power control of wind turbines in grid-forming mode

Bashar Mousa Melhem[1] and Steven Liu[2]

[1] Institute of control systems
Kaiserslautern-Landau Technical University
67663 Kaiserslautern (Germany)
Phone: +4915753112589, e-mail: melhem@rhrk.uni-kl.de

[2] Institute of control systems
Kaiserslautern-Landau Technical University
67663 Kaiserslautern (Germany)
Phone: +49 (0)631 205 4535/2828, e-mail: sliu@eit.uni-kl.de

**Abstract.** Together with the daily variation of load demand in power grids, the continuous integration of offshore and onshore wind farms to feed the grid with green energy has recently led to a severe frequency stability issue due to the extra variation in the generation side. Hence, wind turbines (WTs), among other renewable energy units are required to regulate their output power to mitigate the fluctuation in generated power and support frequency stability. In this paper, model predictive control (MPC) is implemented in an adaptive way to operate WT in de-loading mode under wind disturbances. In addition, to get comprehensive operation of WTs and meet grid code requirements; we present a new grid-forming controller in the WT rotor side converter to emulate the inherent synchronizing and load sharing property of conventional generators. The limitations of rotor speed and rotor side converter are considered in the proposed control approach.

**Key words.** DFIG, Grid Code Requirements, Adaptive MPC, Primary frequency support, grid stability.

## 1. Introduction

Despite the advantage of supplying the grid with green energy from wind, transmission system operators (TSO) are facing nowadays stability issues in their power systems because of the transition in power generation from synchronous generators (SGs) to wind farms, which associates with a variety of generated power profile due to wind conditions [1]. Hence, the risk of compromising the stability of the grid has become the focus of many researches. The negative impact of WTs on the grid stability can be summarized in two major points: first, a wind turbine works in Maximum power point (MPP) adds more oscillation to the grid frequency and exhausts the other conventional generating units in balancing the power generation-consumption [2]. Seconds, considering the fact that grid-following (GFL) control strategy is implemented in most power converters, the presence of a robust grid where frequency and voltage are imposed by SGs is still required to avoid losing the synchronization within the power grid. To overcome this issue, grid-forming (GFM) strategy has to be considered in some interconnected wind turbines to enhance the reliability of the power grid.

In these networks codes (NC RfG EU 631/1447 in 2016 &1485 in 2017), TSOs have clarified in their frequency defence plan that all existing and newly integrated power-generating units with capacity $\geq$ 50MW should respond to grid frequency changes by adjusting their output poweraccordingly. This adjustment applies to both synchronous power-generating modules (SPGM) and renewable power-park modules (PPM) [3]. In the literature, TSO refers to this service as a frequency containment reserve (FCR). Inthis regard, many authors suggested modifying the rotor side converter of wind turbines with Maximum power point tracking operation (MPPT). This modification aims to achieve short-term support following any frequency event by converting a part of kinetic energy in the rotor to active power and injecting it into the grid or vice versa [4],[5]. In the literature, this modification is referred to as synthetic inertia. However, this temporary frequencysupport can be reasonable only in a case where the shareof conventional generators in the grid is sufficient to hand over grid frequency stabilization efforts after any load increase or generator outage scenarios. Based on forthcoming strategies to increase the share of renewable energy generators at the expense of conventional ones, theshort-term frequency support scenario from WT can be problematic. To bridge the gap between the intended transition to green energy and the lack of power reserve due to the reduction in SGs, some authors suggested operating wind turbines in de-loading mode. De-loading operation can be achieved by shifting the operating point below the MPP. Thus, converting a part of the available power from the wind to kinetic energy and storing it in therotor [6], [7]. In this case, wind turbines can increase their output power following any frequency disturbance by converting the additional stored kinetic energy, whetherpartially or entirely to active power and sending it to thegrid. This could be simply achieved mechanically by modifying the pitch controller, or electrically by adjusting the electrical torque in the rotor side converter. However, it is essential to note that considering gird code requirements requires taking additional points into account when applying primary frequency support features in wind turbines. Some of these points are the response time, available power, quality of power delivered into the grid, and the limitations on wind turbine rotor speed and rotor side converter to avoid the unsafe operation of the wind turbine. In [8], [9], the standard/economic MPC is used to maximize wind turbine output power. However, in this paper, the MPC technique is employed to achieve de-loading operation by following the power set-point provided by TSO. First, the optimum operating point of WT is determined based on an adaptive MPC algorithm considering the variations on generation and load sides. The active power control of WT will be carried out at the TSO level. The benefit of it is that it requires only a minimum set of measurements from WT, and it is possible to exploit the adaptation and prediction property of the used control strategy based on the live observed grid status by TSO. Second, a grid-forming approach inspired by the innate response of synchronous generators is applied to get a comprehensive strategy for wind turbines to react as close as possible to SG and hence, follow up the new grid code requirements regarding frequency support. pitch control is not a apart of the proposed control strategy and used here only to limit rotor speed for high wind speed.

## 2. Operation principle of DFIG wind turbine (De-loading operation)

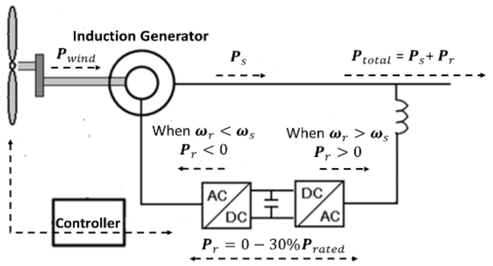


Fig. 1. DFIG wind turbine connected to grid.

The basic model of grid connected DFIG is shown in Fig. 1. This type of wind turbine injects up to 70% of its rated power $P_{wt}^{n}$ into the grid through its stator winding $P_s$ and up to 30% in both directions through its rotor winding $P_r$ to keep voltage of WT synchronized with the grid (rotates at the synchronous speed $\omega_s$). The rotor side converter (RSC) controls the rotor speed to extract the maximum available power from the wind as shown in Fig.2. This can be done by adjusting the electrical torque in theDFIG.

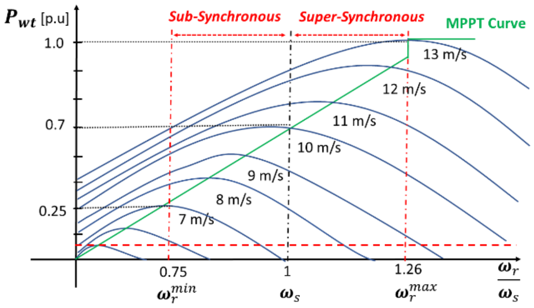


Fig. 2. DFIG WT in MPP operation.

During the de-loading operation, the DFIG WT is not operated along the maximum power point tracking (MPPT) curve but actively along some tracks below the MPPT curve (marked in red in Fig.3) in order to store that part of available wind energy (as reserve) in the form of rotating kinetic energy. This reserved kinetic energy is seen as an increase in rotational speed for the same wind curve. Hence, a de-loading operation is limited by the maximum rotor speed provided in the technical data from the wind turbine manufacturer.

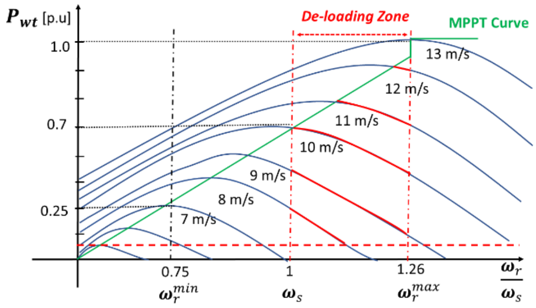


Fig. 3. DFIG WT in de-loading operation.

As shown in Fig.3, the de-loading zone locates below the green MPPT curve and between the minimum allowed rotor speed for de-loading operation ($\omega_s$) and maximum allowed rotor speed $\omega_r^{max}$. $P_{wt}$ could be reduced by a maximum 30% (or 0.3 p.u) and stored as kinetic energy in the rotor. Along with output power de-loading, the rotor speed increases accordingly up to ≈1.26 p.u. It should be highlighted that the operating point (wind speed) plays here an important role in determining the maximum possible de-loading rate or reserve amount in MW, as the output power cannot always be reduced by 30% due to the maximum/minimum allowed rotor speed ($\omega_s$, $\omega_r^{max}$) to avoid the unstable operation of WT.
The table below compares the operating regions of normal and de-loading modes of a 2MW DFIG wind turbine.

Table I. – Limitations of WT in normal and de-loading modes

| WT Operating Region | | | | |
|---|---|---|---|---|
| | Normal Operation | | De-loading | |
| Variable | min | max | min | max |
| $\upsilon_w$ $[m/s]$ | 7 | 13 | 10 | 13 |
| $\omega_r/\omega_s$ | 0.75 | 1.26 | 1 | 1.26 |
| $P_{wt}$ $[p.u]$ | 0.25 | 1 | 0.7 | 1 |

## 4. Dynamic model of DFIG WT

### A. Aerodynamics

Following the best estimation of power coefficient $C_p$, the part of the power stored in the Wind turbine's air cylinder that could be extracted and provided to the grid is given as:

$$P_{ava} = \frac{1}{2}\rho\pi R^2 \upsilon_w^3 C_p(\lambda(\upsilon_w, \omega_r), \beta) \quad (1)$$

Where R is the rotor radius, $\beta$ is the blade pitch angle, $\omega_r$ is the rotor speed, $\upsilon_w$ is the measured wind speed, $\rho$ is the air density, and $\boldsymbol{\lambda}$ is tip speed ratio defined as: $\lambda = \frac{|\omega_r R|}{\upsilon_w}$.

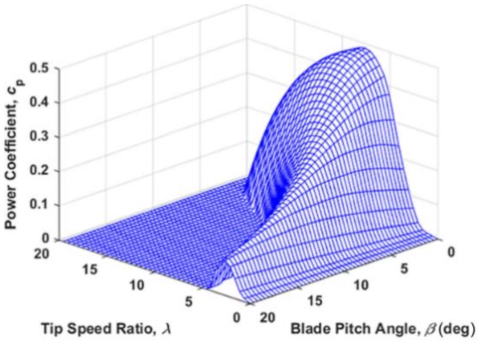


Fig. 4. Power coefficient surface of wind turbine

*B. Active power control at TSO level*

The electrical power response of wind turbine $P_{wt}$ to the aerodynamic power is given as:

$$P_{wt}^{\cdot} = \frac{1}{\tau}\left[P_{ava}\left(\upsilon_w, C_p\right) - P_{wt}\right] \qquad (2)$$

τ: is associated with the drivetrain dynamics.
Based on the available power $P_{ava}$ and wind condition, TSO defines the amount of available power to be maintained as a reserve ($P_{res}$) and hence, provides MPC controller with a power set-point $P_{TSO}^{set}$. Ultimately, based on $P_{wt}$, $P_{res}$, MPC determines the corresponding operating point and passes it to RSC to adjust the rotor speed accordingly. The additional role of MPC here is to reject the fluctuations and disturbances in wind speed and tower-deflection rate $\upsilon_t$ on the linearized WT model to attain better control.

## 5. Adaptive MPC approach for WT de-loading control

The regulation of $\boldsymbol{\omega_r}$ in a comprehensive way to follow the active power set-point is done here using the MPC control algorithm. The adaptive MPC strategy fits the purpose of the research perfectly. It addresses a simplified model of the system for predicting the optimal input/output trajectories (i.e., $\Delta C_{P,k}$ and $P_{wt,k}$) over the prediction horizon $N_P$. The adaptive feature is essential here to handle the inaccuracy in the linearized WT model (due to $\upsilon_w, \upsilon_t$ fluctuation) by updating the prediction model accordingly based on local measurements only. The paper studies WT operating in the region (2) where the rotor speed is below its maximum value $\omega_{r,k} < \omega_r^{max}$ and $\beta = 0$.
The power set-point $P_{TSO}^{set}$ for the MPC controller is provided from TSO based on the generation-load profile.

*A. Prediction model*

*1) Prediction model*
The WT model represents the dynamic power of individual wind turbines that experience turbulent wind flow and wakes at each time instant k.

$$\begin{bmatrix} P_{1,k+1} \\ \vdots \\ P_{n,k+1} \end{bmatrix} = \begin{bmatrix} A_{1,k} & \cdots & 0 \\ \vdots & \ddots & \vdots \\ 0 & \dots & A_{n,k} \end{bmatrix} \begin{bmatrix} P_{1,k} \\ \vdots \\ P_{n,k} \end{bmatrix} + \begin{bmatrix} B_{1,k} & \dots & 0 \\ \vdots & \ddots & \vdots \\ 0 & \dots & B_{1,k} \end{bmatrix} \begin{bmatrix} u_{wt1,k} \\ \vdots \\ u_{wtn,k} \end{bmatrix} \qquad (3)$$

Applying forward Euler method to discretize eq. (1) and eq. (2) with $\Delta t$, yields:

$$A_{i,k} = 1 - \frac{\Delta t}{\tau_{i,k}} \qquad (4)$$

$$B_{i,k} = \frac{1}{2} R^2 \pi \rho \upsilon_{eff}^3 \frac{\Delta t}{\tau_{i,k}} \qquad (5)$$

$\upsilon_{eff}$: is the effective wind speed applied on the blades $\upsilon_{eff} = f(\upsilon_w, \upsilon_t)$.

*2) Optimal control problem*
Minimize the power reference tracking error of wind turbine over a finite time prediction horizon $N_P$ by adjusting the operating point $u_{wt,k}$.

$$min \sum_{k=1}^{N_P} \left[P_{ref} - P_{wt_k}\right]^2 \qquad (6)$$

s.t. $P_{k+1} = A_k P_k + B_k u_{wt,k}$

*B. Solving the optimization problem*

- The prediction model has a parameter-varying nature due to the dependency of $P_{wt}$ on $\upsilon_w$.
- The effective wind speed $\upsilon_{eff}$ is estimated at each sample time (k=0.5) using two local measurements, namely: wind speed $\upsilon_w$ and tower deflection rate $\upsilon_t$.

*C. Receding horizon control law $N_u$*

- The first part of the optimal solution is applied to WT over $N_u < N_P$=5 to regulate its output power to follow $P_{ref}$.
- $u_k = \Delta C_{P,k}$ is translated to rotor speed set-point $\omega_r^{set}$ when passed to the WT local controller.
- $N_u$ is determined so, that MPC reacts to varying atmospheric and operating conditions ($N_u = 2$).

*D. Constraints and limitations*

The following constraints are considered during the design phase of the controller regarding WT operational limits and required response to frequency events according to EU-grid code requirements.

*1) Output power limitations (soft constraints)*
- De-loading rate: $\Delta P \in [0 - 30\%]P_{wt}^n$.
- LFSM-O: $\Delta P \geq 50\% P_{wt}^n$ within 2s.

- LFSM-U: $\Delta P \geq 20\% P_{wt}^{n}$ within 5s.

*2) Controller input rate $C_P$ (hard constraints)*
The operating point of WT can be tuned within a specific range given by: $0 \leq C_{P,k} \leq 0.45$ (Betz limit).

*3) Rotor speed limitation (hard constraints)*
rotor speed of WT can vary in the range:
$\omega_r^{min} \leq \omega_r \leq \omega_r^{max}$. For $\omega_r \leq \omega_s$ WT cannot follow the TSO set-point anymore and has to work in V/F Mode to regulate its voltage and frequency at the terminal.
The proposed control strategy is presented in Fig.5.

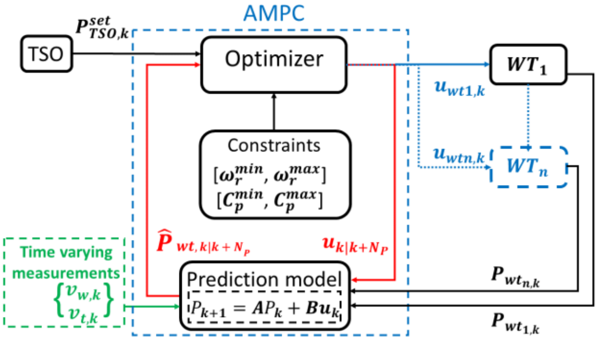

Fig. 5. Block diagram of the proposed adaptive MPC strategy.

The advantage of the adaptive and predictive property of MPC is shown in Fig.6. Two different scenarios are given to illustrate how MPC strategy could be useful to adapt the control input value (operating point $C_P$) to deal with any disturbance on both generation and load sides while following TSO power set-point $P_{TSO}^{set}$.

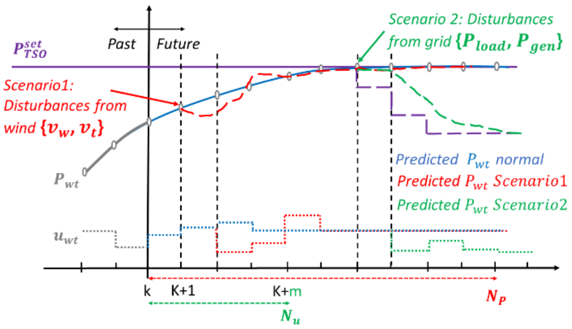

Fig. 6. MPC control strategy for different scenarios.

## 6. Simulation

In Fig.8, 4 different scenarios are simulated, which represent the following cases:

- Constant load and WT in de-loading mode (Ideal case).
- Constant load and WT in MPPT.
- Variable load and WT in MPPT (current actual case).
- Variable load and WT in de-loading mode (intended case).

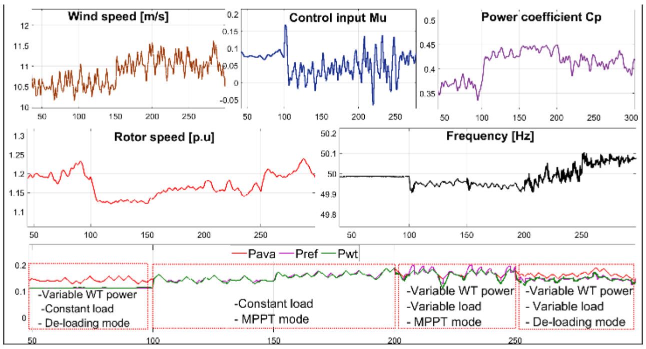

Fig. 7. Simulation results for different scenarios.

As we can see in Fig.7, the frequency is stable at most in case 1, which is, however, never the case since both load and generated power of WT are subject to variations.
Case 4 represents the intended scenario with the proposed control strategy. Simulation results show we can mitigate the frequency oscillation with our control strategy.

## 7. Gird forming operation of WT and synchronization with power grid

To have an optimal integration of WTs in grid frequency support and emulate the role of synchronous generators (SGs) in achieving grid synchronization with the grid properly, WT has to adjust its injected power to the grid within (2-5 sec) following any disturbance as recommended in EU-Grid code.
This could be done by enabling grid forming mode in WT. Nevertheless, before implementing the grid-forming control loop in WT, a short description of how SG achieves synchronization and load sharing is presented.

*A. Synchronization between conventional generators*

The synchronization and load sharing between SGs are done automatically due to their inherent property. The critical factor which ensures that the interconnected SGs react to load disturbance or event homogeneously is the synchronizing power coefficient ($P_s$), which is defined as:

$$P_{s_{ij}} = \frac{V_i V_j}{Z_{ij}} cos(\Delta\delta_{ij_0}) \tag{7}$$

Where $V_i, V_j$ are the terminal voltages, $Z_{ij}$ is the impedance, and $\Delta\delta_{ij_0}$ is the initial phase difference between generators i and j, respectively.
Fig.8 shows a simple example of a grid with 3 SGs to illustrate how SGs react coherently to a load change.

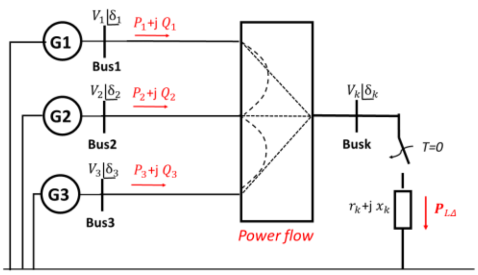

Fig. 8. System topology with 3 conventional generators.

Following any load change ($P_{L\Delta}$) initiated at bus K, all connected generators adjust their injected power accordingly. The response could be summarized in three steps starting from the moment of load change defined as ($t = 0^+$) till the speed governor response ($t_g$):

*1) Electromagnetic response* at $t = 0^+$

- At the moment of load change, no change in the rotor angle of SG occurs due to rotor inertia, i.e., $\delta_{i\Delta} = 0, \delta_{ij\Delta} = 0$. Hence, each SG will sense the phase change at terminal K $\delta_{ik\Delta} = \delta_{i\Delta} - \delta_{k\Delta} = -\backslash delta_{k\Delta}(0^+)$ which is then compensated by the electromagnetic power of SGs. The sensitivity of each SG to $P_{L\Delta}$ depends on the strength of coupling between it and the load, which is represented by the synchronizing power coefficient ($P_{s_{ik}}$).
- The source of the supplied energy is the energy in the magnetic field: $\mathrm{P_{i\Delta}}(0^+) = -\mathrm{P_{s_{ik}}}\delta_{i\Delta}(0^+)$.

*2) Inertial response at* $0^+ < t < t_g$*:*

- The swing equation then takes over the response; the rotor shaft decelerates based on $P_{s_{ik}}$ and $H_i$ as:

$$\mathrm{P_{i\Delta}}(t > 0^+) = \left(\frac{H_i}{\sum_{j=1, j\neq i}^{n} H_j}\right) P_{L\Delta}(0^+) \qquad (8)$$

- The mean frequency deviation is given as:

$$\frac{\mathrm{d}}{\mathrm{dt}}\frac{\mathrm{f_\Delta}}{\mathrm{f_n}} = \frac{-\mathrm{P_{L\Delta}}(0^+)}{\sum_{i=1}^{n} 2\mathrm{H_i}} \ [\mathrm{Hz/s}] \qquad (9)$$

*3) governor response at* $t \geq t_g$

- Rotor speed deviation $\omega_{i\Delta}$ from nominal speed $\omega_n$ is then handed over to the speed governor, which in turn triggers mechanical power change:

$$P_{m\Delta} = \frac{-\frac{1}{2}}{1-\tau_s S}\frac{\omega_\Delta}{\omega_n} \qquad (10)$$

with $\tau_s$ is the turbine time constant.

- Swing equation at this time period is given as:

$$\frac{2H_i s \omega_{i\Delta}}{\omega_n} + \frac{\frac{1}{R_i}}{1+\tau_{si} S}\frac{\omega_{i\Delta}}{\omega_n} = 0 \qquad (11)$$

with $R_i$ is the droop coefficient or regulating strength. The simulation results are seen in Fig.9. after the load increase at t=100s, each generator reacts slightly different to the event based on its own dynamic and distance tothe load. However, all generators stay synchronized as it can be seen from phase angle differences $\delta i - \delta j$ and frequencies $f_i$, and share the load between them. Ultimately, the frequency at each terminal follows the mean frequency, and SGs reach anew operating point within 5 sec after disturbance.

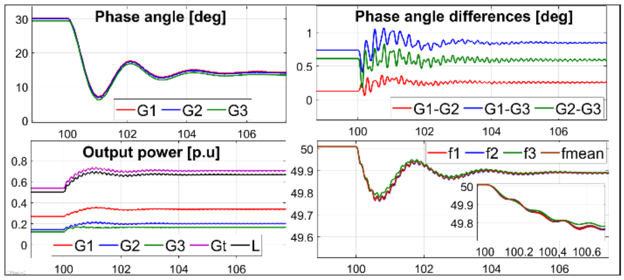


Fig. 9. Simulation results of synchronization between SGs

*B) Proposed Grid-forming control structure for WT*

Since WTs are working in MPPT, they are synchronized to the grid based on the PLL mechanism (GFL). However, by operating them in the proposed de-loading mode, the grid-forming model is then applicable, and WTs can participate in frequency regulation.

*1) Pre-conditions for enabling grid-forming mode in WTs*
An essential condition for operating WTs in grid-forming mode is that they are not working on their maximum limit and have enough reserve to handle the load change $\Delta P_L$. Additionally, $\omega_r$ should not exceed its limits $[\omega_s, \omega_r^{max}]$.

*2) Synchronization between WTs in grid-forming mode*
Similar to SGs, by applying the proper control loops, WTs can synchronize and share the load after any disturbance based on Master-slave logic, where the master WT is the one fitted with a Grid-forming control loop, which in turn, provides PLL loops of slave WTs with reference *V,f.*

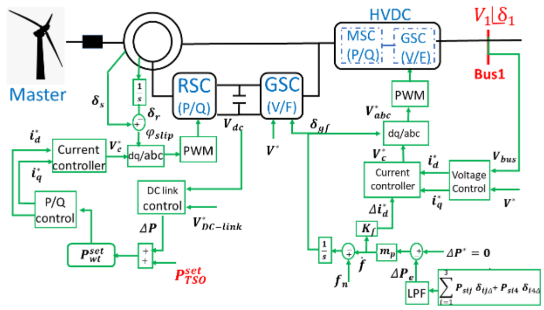


Fig. 10. Grid-forming control strategy in DFIG WT.

The procedure for synchronizing and load sharing is given in the following steps:

- Based on the measured terminal voltages $V_i$ (*i=1,2,3*), $V_k$, the known line impedance between them ($Z_{ik}$) and the initial phase angle difference $\delta_{ij_0}$, the synchronizing power $P_{s_{ik}}$at $t_1 = 0^+$ could be determined.
- The electrical power at Bus i at t=$0^+$ is given as:

$$P_{ik\Delta}(0^+) = \frac{V_i V_k}{Z_{ik}} cos\delta_{ik_0}\delta_{k_\Delta}(0^+) \qquad (12)$$
$$= P_{s_{ik}}\delta_{k_\Delta}(0^+) \qquad (13)$$

- To enable synchronization and load sharing from node i, power change at the terminal i ($P_{i\Delta}(0^+)$) should be provided at $t = t_1 = 0^+ + t_{LPF}$ ($t_{LPF}$ is the time delay by low pass filter for the measured terminal voltages) as a feedback signal to grid side converter (GSC) of master WT:

$$P_{i\Delta}(0^+) = \sum_{j=1,(j\neq i)}^{3} P_{s_{ij}}\,\delta_{ij_\Delta} + P_{s_{ik}}\,\delta_{ik_\Delta} \quad (14)$$

with: $P_{s_{ij}} = \frac{V_i V_j}{Z_{ij}} \cos\delta_{ij_0}, \delta_{1j_\Delta} = \sin^{-1}\frac{P_{ij} Z_{ij}}{V_i V_j}$

and $H_v$ virtual inertia constant.

- As a result, GSC adjusts its PWM reference voltage to allow more current flow to the load. Ultimately, the DC voltage between RSC and GSC will drop. This $\Delta V_{dc}$ will be used then to trigger the DC voltage controller in RSC.

*3) $V_{dc}$ control at RSC at $t \geq t_1$*

- RSC compensates $\Delta V_{dc}$ by adjusting power set-point provided by TSO: $P_{wt}^{set} = P_{TSO}^{set} + \Delta P$.
- The additional required power is determined as $\Delta P = K_d\, V_{dc}$ with $K_d$ as a droop coefficient.

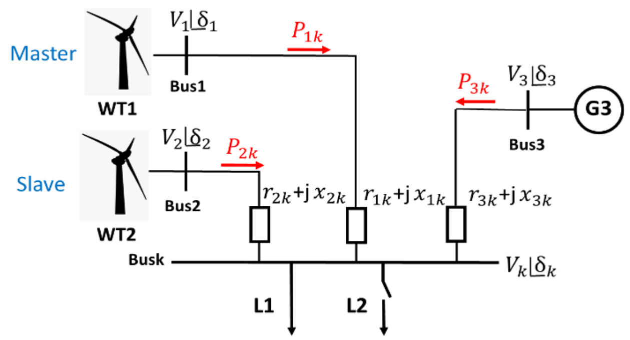


Fig. 11. System topology with 2 wind turbines and one SG.

*4) Simulation results*

The grid topology is given in Fig.11. One SG, one WT in de-loading operation and GFM mode (Master unit), and another WT in MPPT and GFL mode are used. A case study is simulated to see how both WTs react to load change and to verify the de-loading and GFM strategies.7

The simulation results are presented in Fig.12.

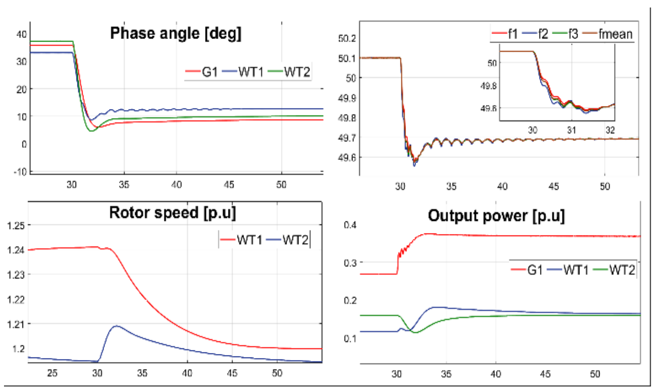


Fig. 12. Simulation results for synchronization between WTs.

## Conclusion

This paper develops a comprehensive, adaptive MPC control for wind turbines to achieve frequency containmentreserve (FCR) and contribute to grid frequency support as recommended in the latest published network codes by operating in de-loading mode and following TSO power

Simulation results verified the ability of wind turbines to emulate the behavior of SG with proper control strategies. A proper GMF strategy inspired by the inherent property of SG is implemented in the WT rotor converter to strengthen the grid's reliability. Further investigation is in the process to generalize the control strategy on more complex grid large-scale wind farms.

## References


[1] V. Vishnuvardhan Yadav, B. Saravanan, "Technical advances and stability analysis in wind-penetrated power generation systems", Fronties in energy research (2022), 10.3389/fenrg.2022.1091512.\\

[2] Innocent O. Ozioko, Nnaemeka S. Ugwuanyi, Arthur O. Ekwue, Charles I. Odeh, "Wind energy penetration impact on active power flow in developing grids" Scientific African (2022),
Volume 18,e01422, ISSN 2468-2276.\\

[3] ENTOSE, "Limited frequency sensitive mode", ENTSO-E guidance document for national implementation for network codes on grid connection (2018).\\

[4] B. M. Melhem, Y. Zhou and S. Liu, "Frequency Support and Stability Analysis for an Integrated Power System with Wind Farms," IECON 2018 - 44th Annual Conference of the IEEE Industrial Electronics Society, (2018), pp. 159-164, doi: 10.1109/IECON.2018.8592707.\\

[5] Alam, M.S.; Al-Ismail, F.S.; Salem, A.; Abido, M.A. High-Level Penetration of Renewable Energy Sources into Grid Utility:Challenges and Solutions. IEEE Access (2020), 8, 190277–190299.\\

[6] A. ZHANG, D. Li, H. XING, Z. WANG and C. SI, "A Robust Reserve Scheduling Method Considering Wind Turbine Generator's De-loading Control," 2019 IEEE 8th International Conference on Advanced Power System Automation and Protection (APAP), (2019).\\

[7] D. Kumar, P. Sharma and H.D. Mathur, "Modified Deloading Strategy of Wind Turbine Generators for Primary Frequency Regulation in MicroGrid", Technol Econ Smart Grids Sustain Energy (2020).\\

[8] Li, X.-M, Zhang, Xi, Lin, Zhongwei, Niu, Y.-G, Li, Mingyang, Nathan, Noel, "Adaptive Multiple MPC for a Wind Farm with DFIG: a Decentralized-Coordinated Approach" (2016),10.5370/JEET.11.5.1116.\\

[9] Song, D., Yang, J., Dong, M., Joo, Y.H, "Model predictive control with finite control set for variable-speed wind turbines". Energy (2017),126:564-572.https://doi.org/10.1016/ j.energy.02.149.\\